JOURNAL OF Materials CHEMISTRY

Strain reduction in supported materials; the formation of cracks and dislocations

Dean C. Sayle

Department of Environmental and Ordnance Systems, Cranfield University, Royal Military College of Science, Shrivenham, Swindon, UK SN6 8LA. E-mail: sayle@rmcs.cranfield.ac.uk

Received 22nd September 1998, Accepted 30th November 1998

Supported materials have been constructed by successively depositing ions onto a surface in conjunction with dynamics simulation and energy minimisation. In particular, the growth of SrO/SrO, CaO/SrO (−6.9% misfit) and BaO/SrO (+7.0% misfit) were studied as model systems to examine the influence of the misfit on the structure and stability of epitaxial thin films. At low (theoretical monolayer) coverage, the CaO formed islands on the SrO(001) surface in contrast to the strips formed by BaO. At higher coverages cracks formed within the CaO, while dislocations appeared within the BaO thin film, in both cases to help reduce the strain within the materials. A mechanism for the formation of the dislocation is presented. For one particular CaO/SrO(001) interface, a cubic–hexagonal transformation of the CaO is observed, enabling the misfit to be perfectly accommodated.

Introduction

The fabrication of high quality crystalline thin film interfaces has become increasingly important recently with applications as diverse as supported superconductors, high density recording media, semiconductor lasers, sensors and catalysis. For many such systems the interface can have a profound effect (beneficial or deleterious) on the properties of the supported material. For example, the interfacial misfit strain energy can be partially accommodated by defects,[1,2] dislocations,[3,4] and grain boundaries[5–8] at the interfacial region which, in semiconductor or superconducting devices, may lead to electrical breakdown.[9] Conversely, such phenomena may enhance certain mechanical properties such as toughness and ductility; the so-called supermodulus effect.[10] In addition, the ability of the substrate to effect the exposure of a particular face or surface reconstruction, resulting in improved physical or chemical properties compared with the unsupported material, has been widely exploited in catalytic systems.[11–13]

Many chemical and physical properties are related to the structural modifications induced into the supported thin films because of interfacial interactions.[14,15] Clearly, an understanding of how such modifications arise and, moreover, how they may be exploited, will aid the design and fabrication of improved materials and considerable progress has been made in these areas.[5,6,10,16–19] Indeed, techniques such as molecular beam epitaxy allow almost atomic level control over the deposition of material on a host substrate.[20,21] However, such techniques can be extremely expensive. Conversely, simulation techniques offer an inexpensive and complementary method with which to study 'model' interfacial systems. In particular, the calculations presented in this study can all be performed on standard PCs.

Perhaps the most powerful aspect of simulation techniques is the ability to systematically investigate simple, but perfectly characterised, model systems and to methodically increase their complexity. It is then possible to deconvolute distinct effects such as the misfit strain energy, the effect of defects or dislocations and the surface preparation of the substrate and correlate these with the interface structure and its chemical, physical and mechanical properties. For example Balducci *et al.*[22] have shown oxygen mobility in CeO_2 increases with Zr doping and Sayle *et al.*[23] found that by interfacing CeO_2 with α-Al_2O_3, the surface oxygen vacancy formation energies in the supported CeO_2 were reduced, with implications for the catalytic activity of ceria. In the latter example, a direct comparison between the interfaced and non-interfaced material enabled the authors to establish directly the effect of the interface on the properties (specifically vacancy formation energies) of the material. Such models of the ceria-based catalysts are very simplistic and other competing factors must be considered. However, these examples illustrate how one can use simulation techniques to adjust a single parameter and monitor its effect. Ultimately, it is desirable to exploit the data to predict conditions which may lead to the fabrication of materials with improved or indeed, optimum properties.

In this present study, we apply simulation techniques to examine the growth and structure of ultrathin interfaces. In particular, to establish the effect of the misfit on the structure of the supported material. Initially, very simple (rocksalt type structure) systems are considered, with a view of extending this to more complex and commercially viable materials in future studies for which a wealth of experimental data is becoming available for comparison.

In a previous study,[24] CaO/SrO thin films were constructed by depositing Ca and O ions onto an SrO support with energy minimisation and dynamics simulation to direct these species into low energy positions. However, to reduce the computational cost, a *rigid* SrO support was used which is likely to influence (artificially) the structure of the resulting thin film. Specifically, the potential field experienced by the deposited ions is not correctly represented if a rigid support is employed as the surface cannot relax in response to the species deposited.[21,25] In this present study, all species, including those comprising the support and overlying thin film, were allowed to relax during the deposition cycles. In addition, the dynamics simulation was run for considerably longer durations than employed previously. Accordingly, in this study, the homoepitaxial growth of SrO on SrO(001) and SrO(510) are investigated, after which the study is extended to include the heteroepitaxial growth of CaO and BaO on SrO(001).

Theoretical methods and potential models

The calculations presented in this study are based on the Born model of the ionic solid in which the ions interact *via* long-range Coulombic interactions and short range, parameterised interactions. Potential parameters for the CaO and SrO were taken from the study of Bush *et al.*[26] In addition, a rigid ion model was used to reduce the computational expense.

All the simulations undertaken in this work, including lattice

and surface construction, energy minimisation and dynamics were performed using the MARVIN code.[27] The program considers the crystal as a stack of planes, periodic in two dimensions and subdivided into two regions: a region I where the ions are allowed to move explicitly, and a region II in which the ions are held fixed relative to each other. Region II may, however, relax as a whole allowing the crystal to either expand or contract. The top of region I is the free surface onto which the species comprising the thin film are deposited. The energy minimisations are all performed at 0 K and therefore the models derived reflect low temperature structures.

To describe adequately the interactions between incommensurate materials, large supercells are required. Conversely, such supercells must also be small enough to be suitably accommodated within the available computational resources available. Therefore, the size of the simulation box was limited to 659 and 672 Å^2 (*i.e.* 10×10 surface lattices) for the SrO(001) and SrO(510) surfaces respectively. In addition, region I for the substrate was limited to two atomic planes for the SrO(001) and 5.5 Å for the SrO(510).

Thin film deposition

To study the growth and structure of the thin film interfaces, the ions comprising the thin film were sequentially deposited onto an SrO substrate until the required thin film thickness was achieved. A small additional program was written to automate this deposition process and was used in conjunction with the MARVIN code, which performed the minimisation and dynamics simulations. The code introduces the ions comprising the thin film, *i.e.* $Sr^{2+}/Ca^{2+}/Ba^{2+}$ and O^{2-} at random positions above the SrO surface and moves them vertically towards the surface until they are within 2.5 Å from the surface or any previously deposited strontium or oxygen species. Energy minimisation and/or dynamics simulation was then applied to the system (comprising the species deposited

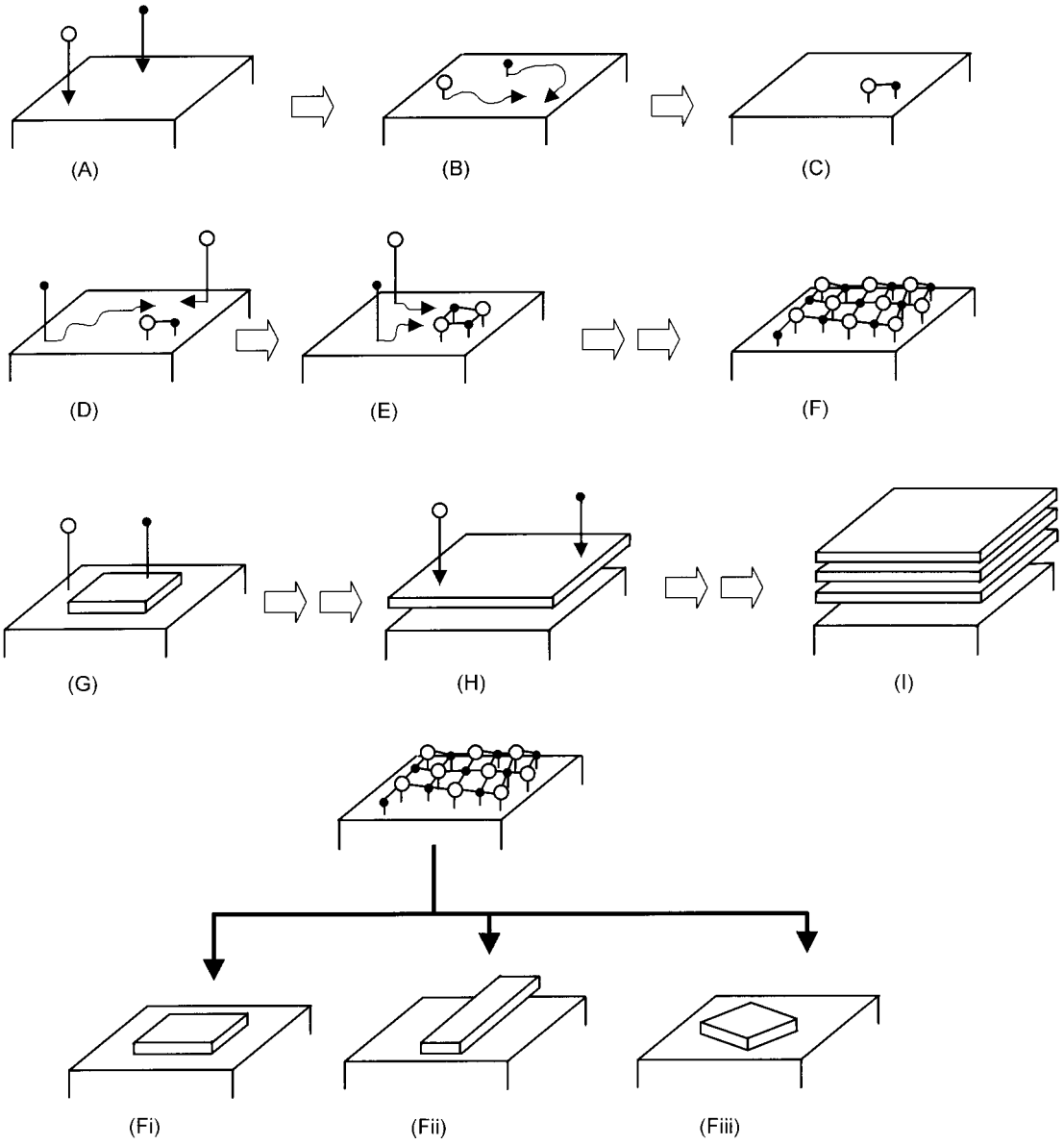

Fig. 1 Schematic of the deposition process: ions comprising the thin films (*i.e.* Ca^{2+} and O^{2-}) are deposited onto the substrate surface (A). Energy minimisation and/or dynamics simulation is then employed to direct these species into low energy configurations (B), resulting in a final structure (C) for the first cycle. Two more ions are then deposited onto the surface and the process repeated (D),(E) until the surface gradually fills with the deposited species (F). After many more deposition cycles (G), (H), the required thin film thickness is reached (I) and the deposition process stopped, after which particular structures (after the deposition of, for example, 50, 100, 150, 200 Ca,O species have been deposited) are considered further: For example (F) represents the case when 9 Ca,O species have been deposited. Long duration dynamics simulation at high temperatures is then applied to this structure and during the dynamics the structure is quenched at regular time intervals to zero Kelvin (energy minimisation) for example after 100, 300 and 600 picoseconds (Fi), (Fii) and (Fiii). These structures are then analysed.

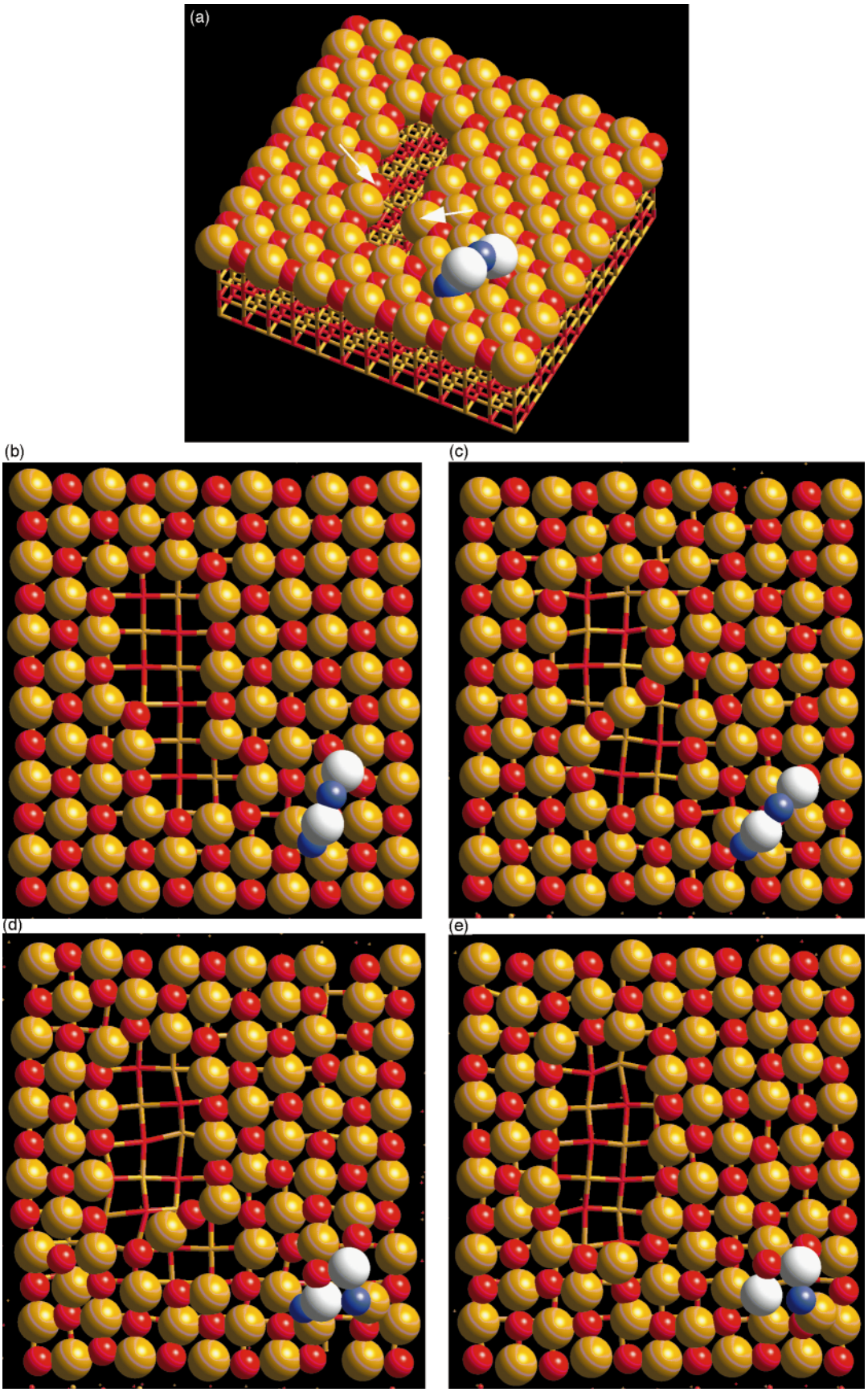

Fig. 2 Representation of the SrO(001) surface after the deposition of 147 SrO species; (a) perspective view which includes two arrows indicating the kink sites on the SrO surface plane; (b–e) snapshots of (a) taken at various time intervals during dynamics simulation. The surface plane is represented by filled balls and the underlying SrO by a stick model. Only part of the SrO support is shown to improve the clarity of the figures. Strontium is coloured yellow and oxygen, red. The additional SrO cluster is highlighted using an alternative colour scheme; strontium is white and oxygen, blue.

and the SrO support) after which, additional species were added and the process repeated until the required thin film thickness was reached. After the deposition process, dynamics followed by energy minimisation (quenching) was performed and the resulting structures were analysed. Fig. 1 illustrates the procedure in more detail.

The quench rate employed in this study was effectively instantaneous, which is likely to influence (artificially) the structure of the thin film when compared with an analogous experimental study. A more appropriate simulation would be to reduce gradually the temperature under dynamics simulation. However, due to the limited timescales possible within typical molecular dynamics calculations, the quench rate would still be much higher than achievable experimentally and, moreover, hugely computationally expensive for such systems.

The stability of each interface was characterised *via* the surface energy, which is given (following Gay and Rohl[27]), by:

$$\gamma_{(hkl)} = [E_{\text{total}}(hkl) - E_{\text{boundary}}(hkl) - nE_{\text{substrate}} - mE_{\text{film}}]/2A(hkl) \quad (1)$$

where γ is the surface energy of the interface; E_{total}, the total energy of the interface; E_{boundary}, the boundary interaction energy; $E_{\text{substrate}}$ and E_{film}, the energy of the perfect crystal comprising the support and overlying thin film respectively; n and m, the number of primitive unit cells within the support and overlying thin film respectively; A, the interfacial area and (hkl) the Miller indices defining the particular surface of the support.

Results

As an initial test of the method, SrO was deposited onto an SrO substrate in order to ensure the method reproduces correctly the bulk SrO structure. Accordingly, SrO species were deposited onto the SrO(001) and the SrO(510), the latter to represent a surface comprising a high concentration of steps. The work was then extended to examine the heteroepitaxial growth of CaO on SrO(001) and BaO on SrO(001). These two systems should provide structural insights into the effect of depositing a material with smaller (CaO) and larger (BaO) lattice parameters compared with the SrO substrate.

SrO/SrO(001)

To examine the homoepitaxial growth of strontium oxide, SrO species were deposited, following the procedure described above, onto a 10×10 SrO(001) substrate: Full monolayer coverage therefore corresponds to the deposition of 50 SrO units.

Fig. 2(a) illustrates the structure after 147 SrO species have been deposited onto the surface followed by 100 picoseconds (ps) of dynamics simulation at 2000 K and a final energy minimisation step. The figure suggests that the SrO species deposited extend the rocksalt structure, while maintaining the exposure of the (001) plane at the surface. The first two planes deposited are completely filled, while the uppermost or surface plane of the figure (illustrated by filled spheres) comprises steps and kink sites, the latter depicted by the two arrows in the figure. These surface ions exhibit reductions in bond distances, characteristic of edge and step species, because of their lower coordination.

During the dynamics simulation snapshots of the structure were inspected at various time intervals. At *ca.* 30 ps, the SrO deposited contained a high concentration of both charged and charge neutral vacancies which were gradually annealed out of the structure during the dynamics simulation. In particular, Sr,O species migrate across the surface to fill vacant sites at lower planes. Indeed, a Sr_2O_2 cluster [Fig. 2(a)] remains on the surface layer even after 100 ps.

To investigate whether this Sr_2O_2 cluster would migrate across the surface to fill four of the vacant positions on the uppermost SrO plane, the dynamics simulation was run for a further 50 ps at 2400 K. Inspection of 'snapshots' of the structure during the simulation [Fig. 2(b)–(e)] suggests that rather than migrate across the surface to fill vacant sites, the cluster rearranged from a linear structure [Fig. 2(b)] to a square planar configuration [Fig. 2(e)]. The latter is expected to be more stable due to the increased coordination of the Sr and O ions. Consequently, the energy barrier for further migration of this cluster to fill the vacant surface sites is likely to be higher and therefore unlikely to be observed under further dynamics simulation due to the limited timescales possible with this technique. To eliminate such 'local minima' problems one may perhaps consider the application of Monte Carlo techniques.[28,29] A mechanism for the intermixing of the ions can also be seen from the snapshots [Fig. 2(b)–(e)]. For example, the final structure [Fig. 2(e)] reveals that the Sr_2O_2 cluster comprises an oxygen from the SrO(001) surface plane (coloured red) rather than from the original cluster (blue): during the dynamics simulation the lattice oxygen (red) is able to migrate out of the surface to coordinate with the overlying Sr_2O_2 cluster, after which, the oxygen originating from the cluster (blue), migrates across to fill the lattice site.

More interestingly, the oxygen and strontium kink sites [illustrated by the arrows in Fig. 2(a)] 'anneal' out during the simulation, the mechanism of which can be seen from Fig. 2(b)–(e): The ions, comprising the kink, initially migrate across the surface to create an Sr–O–Sr–O chain [Fig. 2(c)] which then migrates to eliminate the kink sites [Fig. 2(d), (e)]. In addition, the final structure is 0.05 J m^{-2} more stable than the structure which included the kinks. Such increased stability is attributed to the elimination of the kink sites and the rearrangement of the linear Sr–O–Sr–O cluster to form a square planar arrangement. The surface energy of this final structure was calculated to be 0.67 J m^{-2}, which compares with 0.5 J m^{-2} calculated for a 'perfect' SrO(001) surface. The residual 0.17 J m^{-2} reflects the destabilisation of the surface as a consequence of the surface steps and the additional square planar Sr_2O_2 cluster. Indeed, the surface energy is nearer that

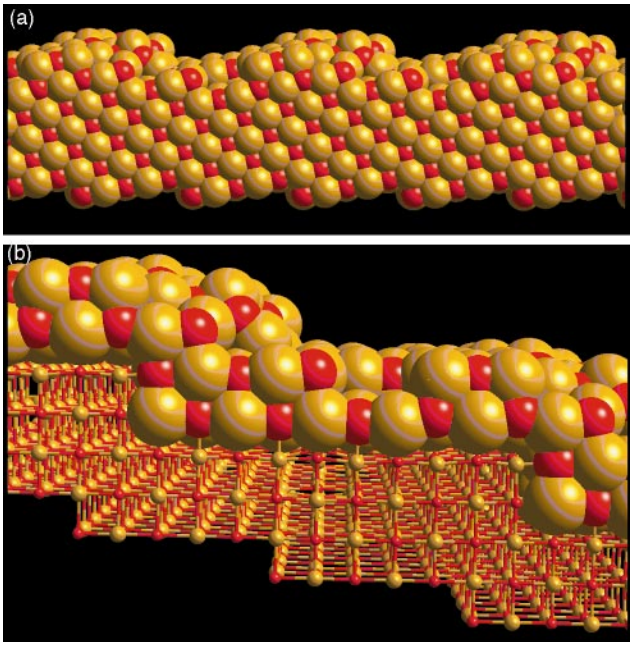

Fig. 3 Representation of the SrO(510) surface after the deposition of 170 SrO species; (a) filled sphere model and (b) filled sphere and ball and stick representation illustrating more clearly the diatomic step. Strontium is coloured yellow and oxygen is red.

calculated for a perfect SrO(510) surface (0.78 J m^{-2}) which is representative of a stepped surface.

SrO/SrO(510)

As a further test of the deposition process and simulation method, the growth and structure of SrO species deposited onto a SrO(510) support, which comprises a high concentration of steps, was investigated.

Fig. 3(a) and (b) illustrate the surface structure after 170 SrO species have been added (3.4 theoretical SrO layers). In accord with growth on the SrO(001) surface, deposition on the stepped surface leads to an extension of the rocksalt structure. Surprisingly, the structure suggests that the growth results in a coalescence of the monatomic steps to form diatomic steps on the surface. The step is not atomically sharp, rather it subtends an angle of about 60° to the [001] direction surface which perhaps suggests the SrO(102) plane (63.4°) although the complex relaxational behaviour of this structure makes such characterisation difficult. The calculated surface energy of this structure is 1.1 J m^{-2}, which is 0.32 J m^{-2} less stable than that calculated for the perfect SrO(510) surface. The surface energy is expected to be higher since the deposition of 170 species does not facilitate a complete surface coverage as discussed above for the SrO(001) surface. Calculations performed by Goniakowski and Noguera[30] on the surfaces of MgO suggest that a diatomic step is energetically more stable than two monatomic steps.

That the procedure is capable of reproducing correctly the structure of SrO promotes confidence in the application of the method to study the growth of heteroepitaxial systems, which is considered in the following sections. In particular, the deposition of CaO and BaO on SrO(001) are investigated. The two systems reflecting the effect of depositing a material with a smaller (CaO, −6.9% misfit) and larger (BaO, +7.0% misfit) lattice parameter compared with the SrO support.

CaO/SrO(001)

Following the procedure described above, CaO species were deposited onto a 10 × 10 SrO(001) substrate and Fig. 4(a)–(d) depict the structures after 50, 100, 150 and 200 CaO species (one to four monolayers) have been added respectively. For 50, 100 and 150 species deposited, dynamics simulation at 2600 K for 300 ps was performed, while for 200 species added, dynamics at 2600 K for 600 ps was run. The latter required about 600 h on a Silicon Graphics O2 with a 150 MHz, R10000 processor. In addition, most of the calculations were performed on standard 300 MHz PCs which were found to perform identical calculations about 10% faster than the Silicon Graphics workstation.

For 50 CaO species added (monolayer coverage) the CaO forms bilayer clusters on the surface of the SrO substrate [Fig. 4(a)] rather than completely filling the surface with a monatomic layer. These CaO clusters adopt a coherent rocksalt type structure while exposing the (001) plane at the surface. Ca–O bond distances within the cluster range from 2.5 Å at the centre of the cluster to 2.1 Å at the edges with an average of 2.3 Å, reflecting the lower coordination of these ions. The interfacial separation is *ca.* 2.4 Å with Ca and O species lying directly above their respective counter-ions of the SrO support.

Since the lattice parameter of CaO (4.79 Å) is smaller than that of SrO (5.13 Å), complete monolayer coverage, with the CaO lying in registry with the underlying SrO(001), would

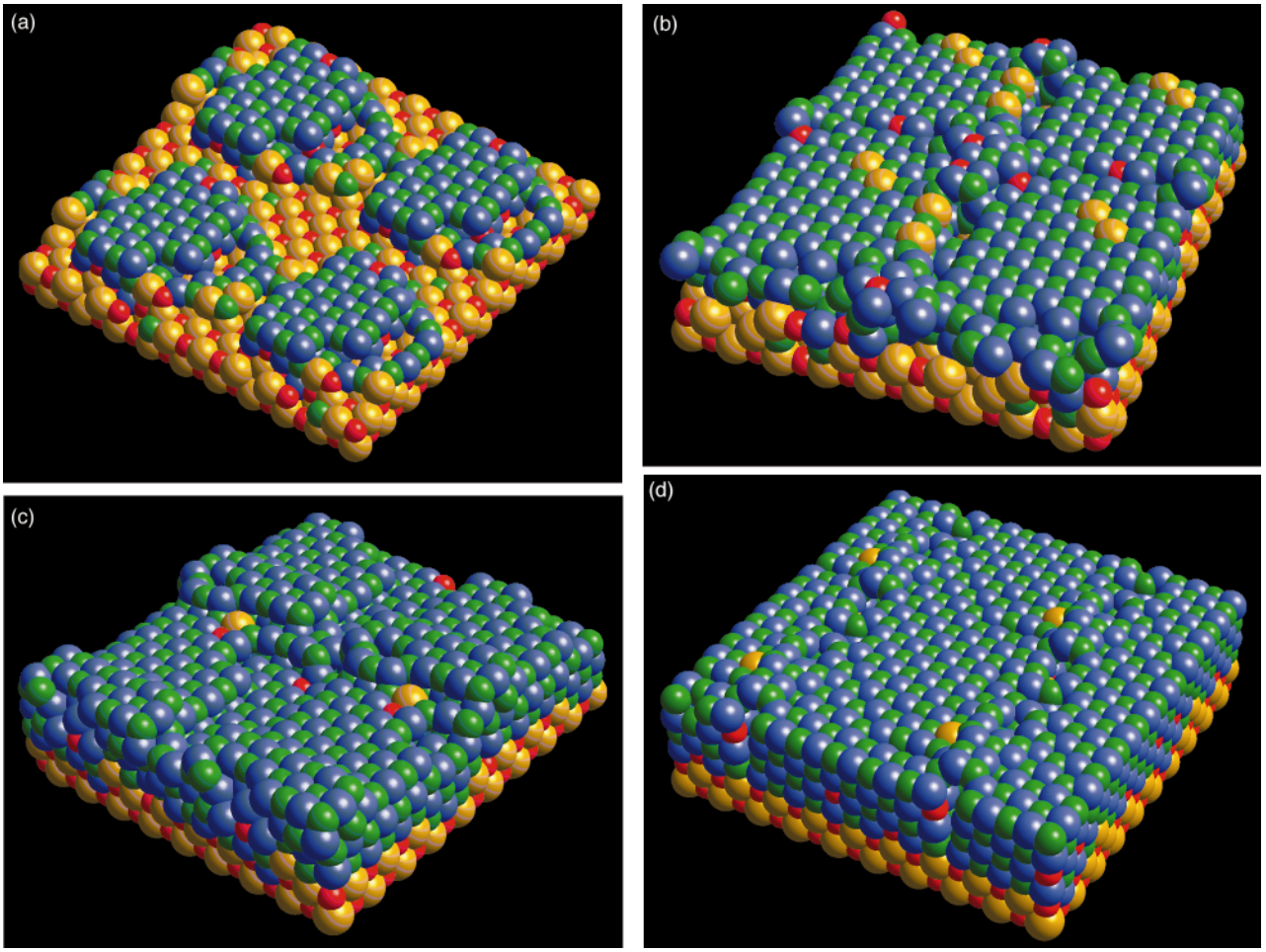

Fig. 4 Representation of the CaO/SrO(001) system after the deposition of (a) 50 CaO species; (b) 100 CaO species; (c) 150 CaO species and (d) 200 CaO species onto the SrO(001) surface. Oxygen (SrO) is coloured red, strontium is yellow, oxygen (CaO) is green and calcium, blue.

require a 6.9% expansion of the CaO lattice resulting in considerable strain within the lattice. The driving force to cluster formation can therefore be attributed, in part, to the reduction in the strain energy. In more general terms one might also reason that similar systems, where the overlying thin film has a lower lattice parameter than that of the support, would also form clusters. While this may indeed be true in many cases, particularly those associated with a large misfit, one must also consider that the energy terms associated with favourable interactions across the interface might outweigh the misfit strain energy.

After 100 CaO species have been deposited, the CaO clusters coalesce to form a bilayer, completely covering the SrO surface [Fig. 4(b)]. The structure of the CaO remains coherent but displays misfit induced structural relaxations. Intermixing of the ions across the interface is also evident; Sr and O ions from the support are present in the surface layer of the CaO thin film and Ca and O ions from the CaO also accommodate lattice positions within the underlying SrO support. In accord with the mechanism for intermixing described for SrO/SrO(001) above, the deposition of CaO onto the SrO surface facilitates the migration of Sr and O species out of the SrO surface plane. These vacant positions may then be filled immediately with Ca,O or remain as vacancies to be filled later during the deposition process. A study by Lind *et al.*[20] on the growth of Fe_3O_4/NiO thin films using molecular beam epitaxy, reveals interfacial diffusion of the Fe_3O_4 and NiO layers of the order of one or two atomic layers.

For 200 CaO species added, the structure is very coherent [Fig. 4(d)]. A side view of a small section of this structure is shown enlarged in Fig. 5(a) and (b), revealing more clearly a 2.8 Å wide 'crack' on the surface of the CaO, the formation of which is attributed to the misfit between the two materials: For example the CaO must accommodate a 6.9% increase in lattice parameter to maintain its registry with the underlying SrO, generating strain within the CaO thin film. The CaO thin film compensates by relaxing in the plane of the interface, resulting in the formation of a crack. The average Ca–O distances in each of the four CaO planes are calculated to be 2.50, 2.43, 2.38 and 2.30 Å for the CaO planes one (interfacial plane) to four (surface plane) respectively; a reduction of about 8% from planes one to four. The crack does not however traverse the entire length of the thin film, rather the crack 'opens' and then 'closes' within the ten planes of the primitive interfacial unit cell.

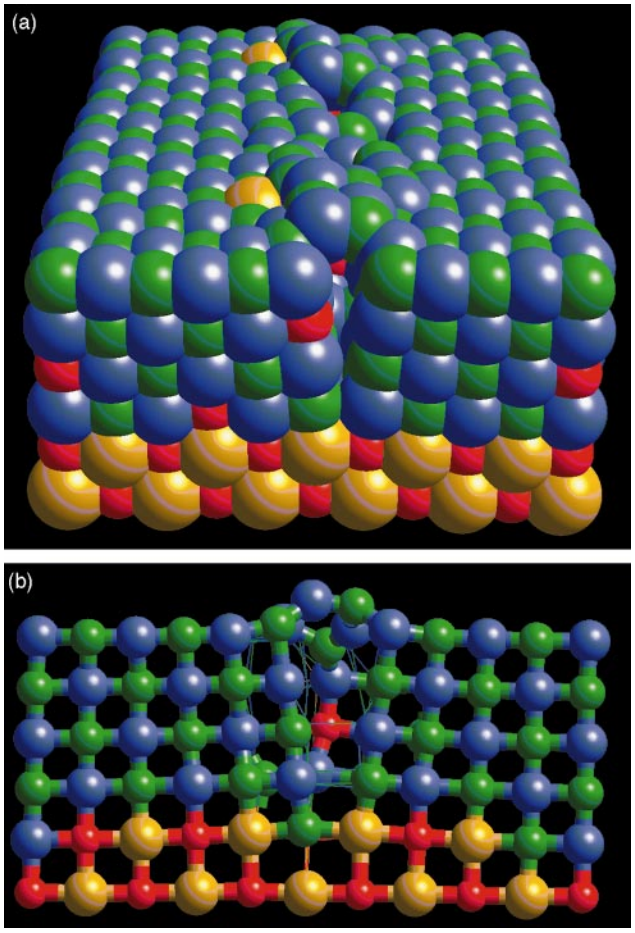

Fig. 5 Representation of a section of Fig. 4(d) illustrating more clearly the 'crack' in the CaO thin film; (a) filled sphere model with perspective; (b) side view illustrating only the foremost ions and the ions directly behind the gap with ball and stick representation.

The presence of a crack in a supported thin film will be associated with a high stress field, which is likely to penetrate deep within the support material. To determine whether the thickness of the SrO support is adequate to describe the relaxation of the ions comprising the support in response to this stress, the thickness of the SrO support (region I) was increased from two to four layers. That the resulting displacement of planes three and four, after the system was energy minimised, were effectively zero and the structure of the 'crack' remained unchanged, suggests the thickness of the support is sufficient. A more convincing approach would be to repeat the deposition of the CaO on a thicker SrO substrate. However, such a calculation is, at present, computationally prohibitive.

Crack formation in supported materials is well known and is almost always detrimental to their particular application.[31] A greater understanding of how cracks occur and, moreover, how they may be reduced or eliminated, will clearly aid the fabrication of improved devices. For example the $YBa_2Cu_3O_{7-\delta}$ has a tendency to crack along the (001) planes in epitaxial thin films of $YBa_2Cu_3O_{7-\delta}(110)/SrTiO_3(110)$ and Olsson *et al.* have used transmission electron microscopy to view these cracks which extend from *ca.* 10 Å near the interface to *ca.* 100 Å at the surface.[32] The authors suggest that these cracks form as a consequence of the thermal expansion mismatch during the cooling process and have proposed, with excellent agreement with experiment, a theoretical analysis of the crack spacing with critical thin film thickness. Similarly, for the simulated thin films in this present study, the quenching (energy minimisation) from high temperature dynamics simulation may have resulted in such a crack within the thin film. However, further study is required to identify how such cracks may be reduced or indeed eliminated.

During each of the dynamics runs the structures were energy minimised at regular time intervals (quench dynamics) to monitor the structure of the 'evolving' thin film during the dynamics (see Fig. 1). One particular structure, comprising 200 CaO species, was calculated to be particularly stable and is illustrated in Fig. 6. For this interface the CaO overlayer adopts a hexagonal, as opposed to a cubic structure which allows the CaO to accommodate perfectly the misfit: a transformation from cubic to hexagonal surface symmetry facilitates an increase in the surface area and consequently the misfit may be eliminated. In particular, based on geometrical arguments, a change from cubic to hexagonal symmetry would be associated with an increase in surface area of about 26%. Moreover, by introducing a partial deviation from cubic to hexagonal symmetry into the structure one could, theoretically, achieve any value between these limits, enabling the misfit to be perfectly accommodated. The resulting structure (Fig. 6) supports this argument by displaying almost perfect coherence within the CaO thin film with no observable (strain-induced) structural modifications. In this case the CaO does not adopt 'perfect' hexagonal surface symmetry which is reflected in a 6% reduction in the Ca–O bond distances and O–Ca–O bond angles ranging from 97 to 157°.

A theoretical study by Recio *et al.*[33] suggests that for small

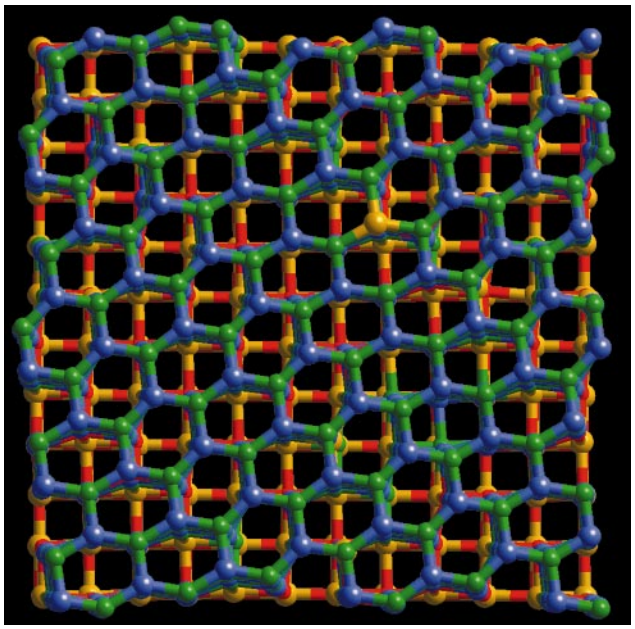

Fig. 6 Ball and stick representation of 4 layers of CaO/SrO(001) looking down on the surface of the thin film. Oxygen (SrO) is coloured red, strontium is yellow, oxygen (CaO) is green and calcium blue.

$(Mg_3O_3)_n$ clusters, hexagonal rather than cubic symmetry is energetically favourable for small values of n. As n increases, the energy difference is reduced until the cubic structure becomes energetically favourable. It is expected that such phenomenon would be observed for other materials which display the rocksalt type structure, such as CaO. Accordingly, the calculations in this present study suggest that for the CaO/SrO(001) thin film, the energy cost in transforming the CaO from cubic to hexagonal surface symmetry is outweighed by the strain energy associated with accommodating the lattice misfit. Whether, at a particular 'critical thickness', the CaO will revert back to the cubic structure could not be deduced and therefore it must be noted that this particular interface structure is an appropriate model for only ultrathin films.

The surface energies of the interfaces comprising one to four CaO layers on the SrO(001) substrate are presented in Table 1. The energies show a decrease in stability with increasing layers, which is attributed to the strain energy associated with each additional CaO plane deposited. However for four layers of CaO on SrO(001), the hexagonal form (Fig. 6) is more stable than the cubic structure [Fig. 4(d)]. Indeed, it is of equivalent stability as a monolayer of CaO on SrO [Fig. 4(a)]. Such stability is attributed to the ability of the CaO to undergo a transformation from cubic to hexagonal symmetry thereby eliminating the misfit as argued above.

To examine further the influence of the misfit on the structure of incommensurate interfaces, the deposition of BaO on SrO(001) is considered. For this system, the BaO thin film has a 7% larger lattice parameter compared with that of the SrO support.

Table 1 Calculated surface energies for SrO/SrO(001), SrO/SrO(510), CaO/SrO(001) and BaO/SrO(001)

	Surface energy/J m^{-2}	Fig.	Final dynamics step/ps
SrO/SrO(001)	0.67[a]	2(e)	150
SrO/SrO(510)	1.10	3(a, b)	100
CaO/SrO(001)			
1 Layer	0.90	4(a)	200
2 Layers	0.97	4(b)	300
3 Layers	1.05	4(c)	250
4 Layers	1.09	4(d)	600
4 Layers (Hexagonal symmetry)	0.90	6	500
BaO/SrO(001)			
1 Layer	0.88	7	225
2 Layers	1.12	8(a, b)	300
3.2 Layers (160 BaO)	1.28	12(a, b)	700

[a]This energy refers to the structure, depicted in Fig. 2(e), after energy minimisation.

BaO/SrO(001)

In accord with deposition of CaO on SrO, a 10×10 SrO(001) surface was used as a substrate to examine the growth and structure of BaO/SrO(001) thin films. Fig. 7 shows the structure of the thin film after 50 BaO species (monolayer equivalent) have been added to the surface. The resulting BaO thin film comprises 'strips' of BaO lying along the [100] direction of the SrO support, in contrast to the clusters observed for CaO/SrO(001). In addition there is a partial filling of a second layer of BaO on the strip. Mixing of ions across the interface is also evident.

For 100 BaO species added [Fig. 8(a), (b)], one can observe clearly defined steps on the surface of the BaO. Closer inspection of the structure reveals that these steps are not just a consequence of creating an additional BaO layer during the deposition process, but indicate the presence of a periodic array of interfacial dislocations within the BaO. The driving force to such behaviour is to reduce the misfit between the SrO support and BaO thin film. For example the lattice misfit associated with lattice matching BaO(5.5 Å) with SrO(5.13 Å) is *ca.* +7%. If a dislocation (removal of one plane of BaO) were introduced into the BaO thin film every ten BaO planes as Fig. 8(a) depicts, the misfit would be reduced to *ca.* −3%, *i.e.* 9 BaO planes matched with 10 SrO planes. The calculations therefore suggest that the energy associated with reducing the misfit by 4% (absolute difference between the +7% and −3% misfits) is sufficient to accommodate the defect energy of the dislocation array. Moreover, the calculated strain energy associated with compressing the lattice by 4% is 0.3 J m^{-2}, which must be larger than the defect energy associated with the dislocation array.

For surfaces, the misfit must be accommodated in two dimensions and therefore it might be expected that dislocations, perpendicular to the ones observed in Fig. 8(a), would be present. However, for this system this is not the case. Instead, the thin film comprises a void of ions on the plateau region [highlighted by an arrow in Fig. 8(b)] which allows the ions to relax in the plane of the interface thereby alleviating the strain in this perpendicular direction. The BaO can there-

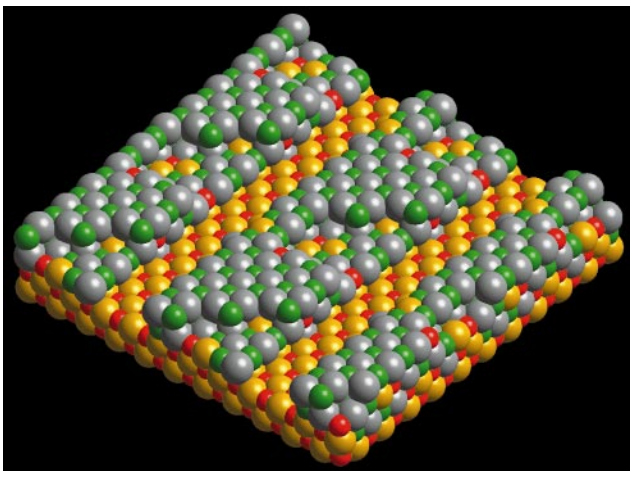

Fig. 7 Perspective view of 50 BaO species deposited on an SrO(001) substrate. Barium is coloured grey, oxygen (BaO) is green, strontium is yellow and oxygen (SrO) is red.

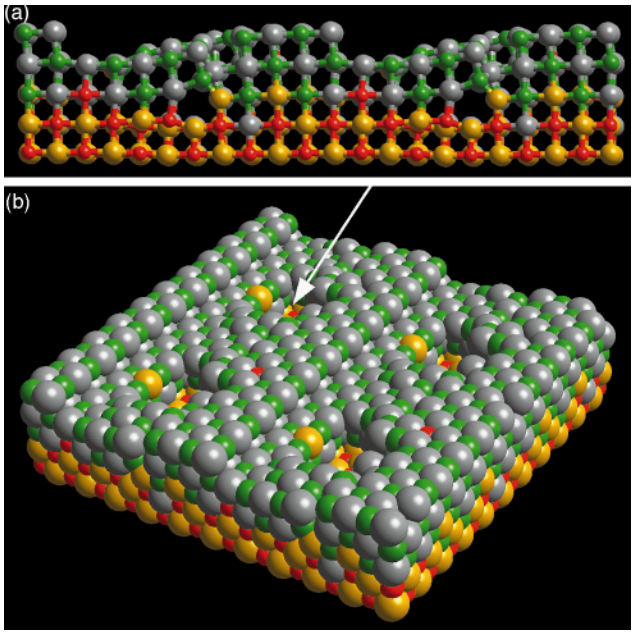

Fig. 8 Representation of the BaO/SrO(001) interface with 100 BaO species deposited, illustrating the dislocation in the BaO thin film; (a) side view; (b) perspective view with an arrow indicating the void in the BaO thin film. Barium is coloured grey, oxygen (BaO) is green, strontium is yellow and oxygen (SrO) is red.

fore be described as the BaO(109)/SrO(001) with the BaO subtending an angle of 6.34 degrees to the SrO(001) surface (Fig. 9).

Evidence of perpendicular dislocations were indeed observed [during the dynamics simulation and quenching procedure [see Fig. 1)] after the deposition of 160 BaO species and are illustrated in Fig. 10 and 11. The arrows in Fig. 10 and 11 highlight the steps in the plane of the surface, which indicate the presence of the dislocations. However, these dislocations proceeded to be annealed out under further dynamics simulation resulting in a structure [Fig. 12(a) and (b)] with dislocations in only one surface dimension. Inspection of the structure (Fig. 12) reveals the void [observed in Fig. 8(b)] is retained, enabling the dislocation to be annealed out of the structure by reducing the strain energy within the thin film.

The formation of misfit dislocations within thin films is supported by a wealth of experimental data (for example ref. 3). In addition, Narayan *et al.*[4] have analysed the formation of strain induced dislocations within $YBa_2Cu_3O_{7-\delta}$ and find that the dislocations, generated at the free surface, move towards the interface to minimise the strain energy of the system. For superconducting devices, the generation and propagation of dislocations must be controlled to reduce the deleterious effect they have on the electrical conductivity.[9] Knowledge of how such dislocations form is a first step in understanding how the dislocation concentration may be

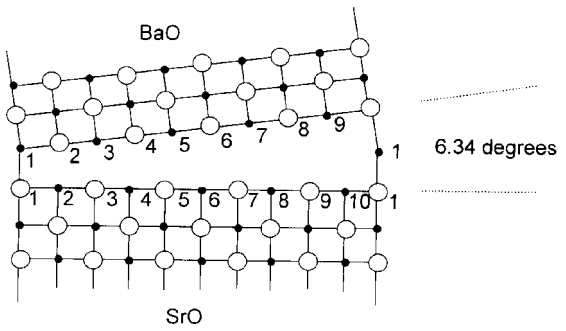

Fig. 9 Schematic of the structure presented in Figs. 8(a) and (b).

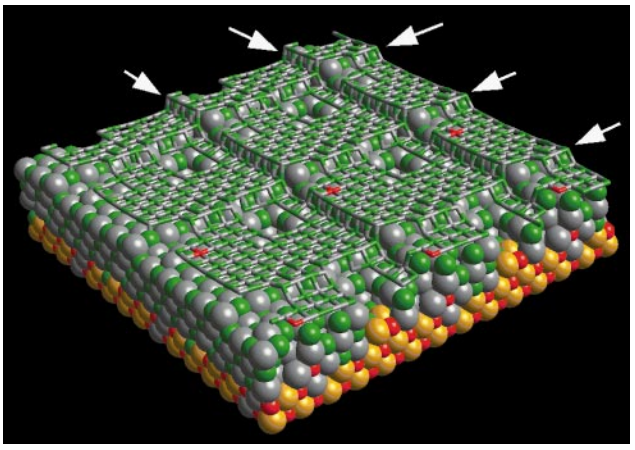

Fig. 10 Representation of the BaO/SrO(001) interface with 160 BaO species deposited. A stick model represents the uppermost BaO layer, while the underlying BaO and SrO are represented by filled spheres. The arrows indicate the orthogonal steps on the BaO surface. Barium is coloured grey, oxygen (BaO) is green, strontium is yellow and oxygen (SrO) is red.

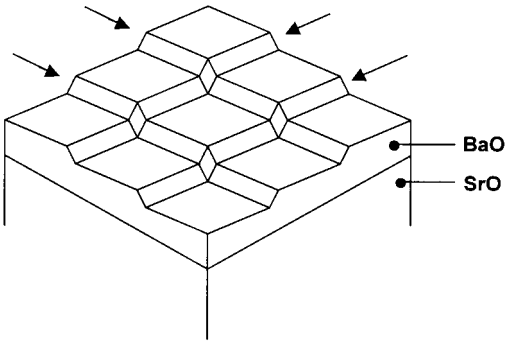

Fig. 11 Schematic of Fig. 10 to aid interpretation of this structure. The arrows indicate the orthogonal steps on the surface.

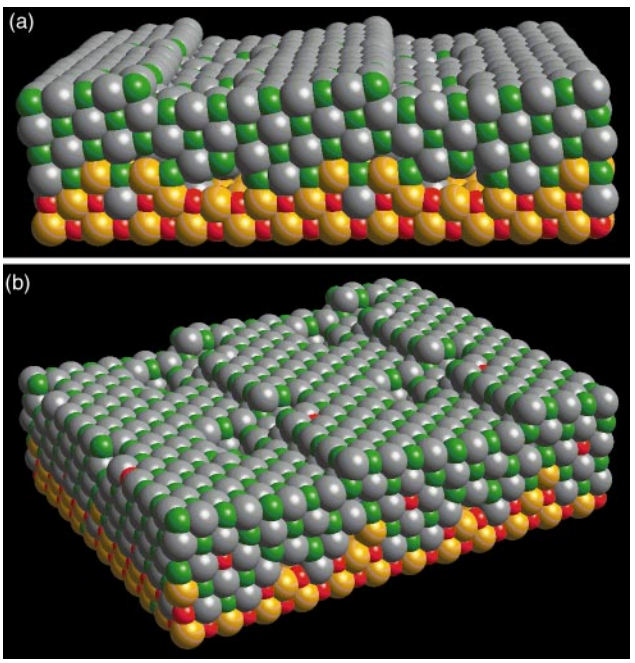

Fig. 12 Representation of the BaO/SrO(001) interface (Fig. 10) after further dynamics simulation; (a) side view with perspective illustrating the dislocation; (b) corner view with perspective. Barium is coloured grey, oxygen (BaO) is green, strontium is yellow and oxygen (SrO) is red.

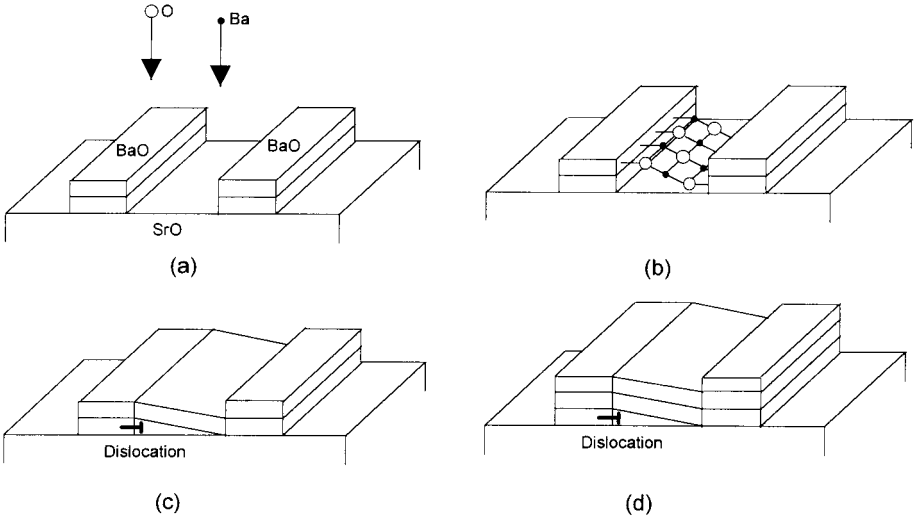

Fig. 13 Schematic illustrating the mechanism of dislocation formation.

reduced, or even eliminated within such films and is addressed in the following section.

Dislocation formation mechanism

Analysis of the structures generated during the deposition of BaO on SrO(001) reveals how the dislocation in the BaO is formed. Fig. 13 illustrates very simply the process: Initially, the BaO deposits on the SrO(001) to form bilayer strips on the surface [Fig. 12(a) and 7]. Upon further BaO deposition, some of the BaO fills the gaps between the strips adjoining the second BaO plane of one strip with the first BaO plane of the other strip [Fig. 13(b), (c)] resulting in the dislocation. Further deposition of BaO leads to an extension of the BaO thin film [Fig. 13(d)].

Fig. 14 illustrates the deposition in more detail. Fig. 14(a) depicts (side view) the two BaO strips on top of the SrO(001) substrate (only three ions in each strip are shown for clarity). The introduction of BaO ions (during further deposition) leads to the filling of the gap between these two BaO strips. Two structures, maintaining charge continuity, are possible [Fig. 14(b) and (c)]. In Fig. 14(b), three ions connect the second plane of one strip with the first plane of the other strip, resulting in the dislocation. As only three (as opposed to four) ions are introduced, there is a large distance between the ions and therefore the strain within the BaO is easily accommodated. However, in Fig. 14(c), four ions fill the gap and to preserve charge continuity must connect the first plane of each strip. Such a configuration, with the BaO in registry with the underlying SrO, generates considerable strain within the BaO lattice and therefore the configuration is energetically less favourable compared with Fig. 14(b). Clearly, an understanding of how such dislocations form will aid the development of new materials with reduced dislocation concentrations.

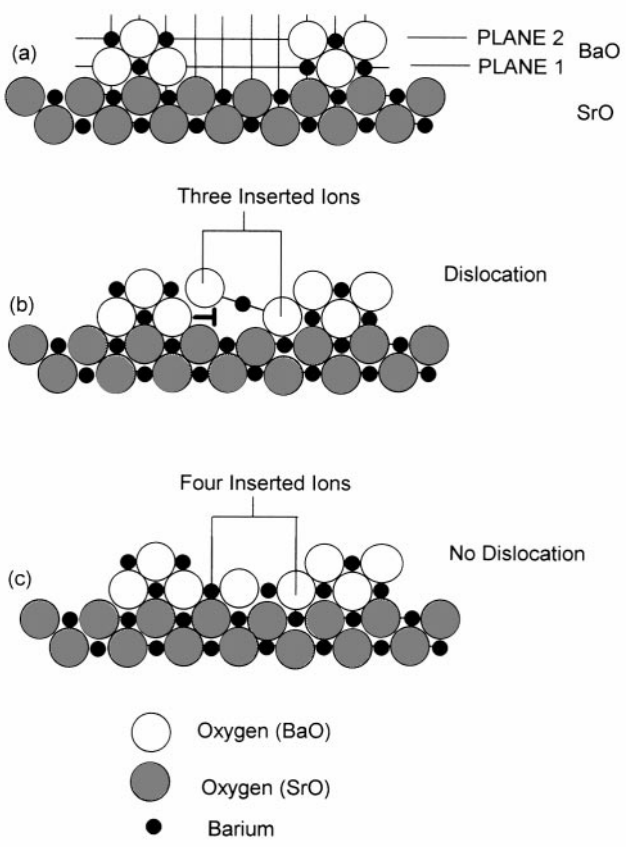

Fig. 14 Schematic illustrating the introduction of three as opposed to four ions within the gap to maintain charge continuity; (a) schematic of the gap [Fig. 13(a)]; (b) introduction of three ions into the gap [Fig. 13(b)] resulting in the dislocation, as opposed to (c), four ions introduced into the gap (resulting in more strain within the system due to the close proximity of the introduced ions).

Conclusion

In this study, thin film interfaces were constructed, *via* the sequential deposition of ions comprising the thin film, onto a substrate surface in conjunction with dynamics simulation and energy minimisation. In particular, SrO, CaO and BaO were deposited on SrO surfaces. The deposition of SrO on SrO(001) (flat surface) and SrO(510) (step surface) was used to determine whether the method could reproduce correctly the SrO structure. For short time-scale dynamics runs, the SrO/SrO(001) structure comprised a high concentration of defects, which, under extended dynamics, at higher temperatures, were annealed out of the structure, resulting in defect free and coherent thin films. In addition the dynamics simulation enabled surface kinks to be annealed out of the structure, increasing the stability of the surface. Deposition of SrO onto a stepped [SrO(510)] surface facilitated a decrease in the concentration of steps; two monatomic steps reducing to a single diatomic step. Such observations are in accord with other theoretical studies, which suggest a diatomic step is more stable than two monatomic steps.

The work was then extended to examine the influence of the misfit on the structure of incommensurate thin film

interfaces. Accordingly, the growth of CaO (−6.9% misfit) and BaO (+7.0% misfit) on SrO(001) were examined. At low deposition levels, (theoretical monolayer coverage) neither the CaO nor the BaO completely covered the SrO with a monatomic thin film, rather the CaO formed bilayer clusters, in contrast to the bilayer strips formed with BaO/SrO.

At deposition levels commensurate with four monolayers, cracks appeared in the CaO thin film, propagating from the interfacial layer to the surface. The crack did not traverse the entire length of the thin film, rather the crack opened and then closed within about seven atomic spacings. In addition, during the dynamics simulation of the four-layer CaO/SrO(001) thin film, the CaO was observed to undergo a transformation from a cubic to a pseudo-hexagonal type structure in the plane of the interface. Such behaviour facilitating an increase in the surface area of the CaO enabling the misfit to be perfectly accommodated, resulting in a very coherent and more stable thin film.

For the BaO/SrO(001) a periodic array of dislocations was formed to help accommodate the misfit. Moreover, by examining snapshots during the deposition process it was possible to present a mechanism for the dislocation formation. Such dislocations are generally deleterious to the material properties and hence reduce the effectiveness of any potential application of the thin film. An understanding of the mechanisms by which dislocations form will therefore aid the development of supported materials with reduced dislocation concentrations.

The study shows how simulation techniques can be applied to examine the structure and stability of thin film interfaces. Moreover, it demonstrates the capability of the method to reproduce rather complex structural changes that may occur within the thin film such as defects, cracks and (rather surprisingly) misfit dislocations and cubic–hexagonal misfit induced transformations.

References

1 O. Eibl, H. E. Hoenig, J.-M. Triscone, O. Fischer, L. Antognazza and O. Brunner, *Physica C*, 1990, **172**, 365.
2 O. Eibl, H. E. Hoenig, J.-M. Triscone, O. Fischer, L. Antognazza and O. Brunner, *Physica C*, 1990, **172**, 373.
3 R. Ramesh, D. Hwang, T. S. Ravi, A. Inam, J. B. Barner, L. Nazar, S. W. Chan, C. Y. Chen, B. Dutta, T. Venkatesan and X. D. Wu, *Appl. Phys. Lett.*, 1990, **56**, 2243.
4 J. Narayan, S. Sharan, R. K. Singh and K. Jagannadham, *Mater. Sci. Eng. B*, 1989, 333.
5 N. Sridhar, J. M. Rickman and D. J. Srolovitz, *Acta. Mater.*, 1996, **44**, 4085.
6 N. Sridhar, J. M. Rickman and D. J. Srolovitz, *Acta. Mater.*, 1996 **44**, 4097.
7 D. M. Hwang, T. S. Ravi, R. Ramesh, S. W. Chan, C. Y. Chen and L. Nazar, *Appl. Phys. Lett.*, 1990, **57**, 1690.
8 T. S. Ravi, D. M. Hwang, R. Ramesh, S. W. Chan, L. Nazar, C. Y. Chen, A. Inam and T. Venkantesan, *Phys. Rev. B*, 1990, **42**, 10141.
9 D. Dimos, P. Chaudhari and J. Mannhart, *Phys. Rev. B*, 1990, **41**, 4038.
10 D. Wolf and J. A. Jaszczak, *J. Comput.-Aid. Mater. Des.*, 1993, **1**, 111.
11 G. Centi, F. Trifiro, J. R. Ebner and V. M. Franchetti, *Chem. Rev.*, 1988, **88**, 55.
12 G. Centi, S. Perathoner and F. Trifiro, *Res. Chem. Intermed.*, 1991, **15**, 49.
13 H. Cordatos, T. Bunluesin, J. Stubenrauch, J. M. Vohs and R. J. Gorte, *J. Phys. Chem.*, 1996, **100**, 785.
14 D. C. Sayle, C. R. A. Catlow, M.-A. Perrin and P. Nortier, *J. Phys. Chem.*, 1996, **100,** 8940.
15 C. Hardacre, R. M. Ormerod and R. M. Lambert, *J. Phys. Chem.*, 1994, **98**, 10901.
16 S. Ramamurthy and C. B. Carter, *Phys. Status Solidi A*, 1998, **166**, 37.
17 M. Kubo, Y. Oumi, R. Miura, A. Stirling, A. Miyamoto, M. Kawasaki, M. Yoshimoto and H. Koinuma, *Phys. Rev. B*, 1997, **56**, 13535.
18 A. M. Stoneham, M. M. D. Ramos and A. P. Sutton, *Phil. Mag. A*, 1993, **67**, 797.
19 S. Bernal, F. J. Botana, J. J. Calvino, G. A. Cifredo, J. A. Perez-Omil and J. M. Pintado, *Catal. Today*, 1995, **23**, 219.
20 D. M. Lind, S. D. Berry, G. Chern, H. Mathias and L. R. Testardi, *Phys. Rev. B*, 1992, **45**, 1838.
21 G. Chern, *Surf. Sci.*, 1997, **387**, 183.
22 G. Balducci, J. Kaspar, P. Fornasiero, M. Graziani, M. S. Islam and J. D. Gale, *J. Phys. Chem. B*, 1997, **101**, 1750.
23 D. C. Sayle, T. X. T. Sayle, S. C. Parker, J. H. Harding and C. R. A. Catlow, *Surf. Sci.*, 1995, **334**, 170.
24 D. C. Sayle, *J. Mater. Chem.*, 1998, **8**, 2025.
25 A. L. Shluger, A. L. Rohl and D. H. Gay, *Phys. Rev. B*, 1995, **51,** 13631; A. L. Shluger, A. L. Rohl and D. H. Gay, *J. Vac. Sci. Technol. B*, 1995, **13**, 1190.
26 T. S. Bush, C. R. A. Catlow and P. D. Battle, *J. Mater. Chem.*, 1995, **5**, 1269.
27 D. H. Gay and A. L. Rohl, *J. Chem. Soc.*, *Faraday Trans.*, 1995, **91**, 925.
28 N. Metropolis, A. W. Rosenbluth, M. N. Rosenbluth, A. H. Teller and E. Teller, *J. Chem. Phys.*, 1953, **21**, 1087.
29 J. Yao, R. A. Greenkorn and K. C. Chao, *Mol. Phys.*, 1982, **46**, 587.
30 J. Goniakowski and C. Noguera, *Surf. Sci.*, 1995, **340**, 191.
31 E. S. Hellman, E. H. Hartford and E. M. Gyorgy, *Appl. Phys. Lett.*, 1991, **58**, 1335.
32 E. Olsson, A. Gupta, M. D. Thouless, A. Segmuller and D. R. Clarke, *Appl. Phys. Lett.*, 1991, **58**, 1682.
33 J. M. Recio, R. Pandey, A. Ayuela and A. B. Kunz, *J. Chem. Phys.*, 1993, **98**, 4783.

Paper 8/07377E